ChemMedChem

Chemistry Europe
European Chemical Societies Publishing

Accepted Article

Title: Inhibition of Human Cholinesterases and In Vitro β-Amyloid Aggregation by Rationally Designed Peptides

Authors: Ivan Sanchis, Roque Spinelli, Jose Dias, Xavier Brazzolotto, Alvaro Rietmann, Florencia Aimaretti, and Alvaro S Siano

To be cited as: *ChemMedChem* **2023**, e202200691

Link to VoR: https://doi.org/10.1002/cmdc.202200691

WILEY VCH

RESEARCH ARTICLE WILEY-VCH

Inhibition of Human Cholinesterases and In Vitro β-Amyloid Aggregation by Rationally Designed Peptides

Ivan Sanchis,[a,b] Roque Spinelli,[a,b] José Dias,[c] Xavier Brazzolotto,[c] Álvaro Rietmann[a,b], Florencia Aimaretti,[a,b] and Álvaro S. Siano*[a,b]

[a] I. Sanchis, Dr. R. Spinelli, A. Rietmann, F. Aimaretti, Dr. A. S. Siano
Department of Organic Chemistry
Faculty of Biochemistry and Biological Sciences
National University of the Littoral
Ciudad Universitaria UNL, 3000 Santa Fe, Argentina
E-mail: asiano@fbcb.unl.edu.ar
[b] I. Sanchis, Dr. R. Spinelli, A. Rietmann, F. Aimaretti, Dr. A. S. Siano
National Scientific and Technical Research Council (CONICET)
Ministry of Science, Technology and Innovation
Godoy Cruz 2290, Ciudad de Buenos Aires, Argentina
[c] Dr. J. Dias, Dr. X. Brazzolotto
Département de Toxicologie et Risques Chimiques
Institut de Recherche Biomédicale des Armées (IRBA)
1 Place du Général Valérie André, 91220, Brétigny-sur-Orge, France

Supporting information for this article is given via a link at the end of the document.

Abstract: The multifactorial nature of Alzheimer's disease (AD) is now widely recognized, which has increased the interest in compounds that can address more than one AD-associated targets. Herein, we report the inhibitory activity on the human cholinesterases (acetylcholinesterase, hAChE and butyrylcholinesterase, hBChE) and on the AChE-induced β-amyloid peptide (Aβ) aggregation by a series of peptide derivatives designed by mutating aliphatic residues for aromatic ones. We identified peptide W3 (LGWVSKGKLL-NH_2) as an interesting scaffold for the development of new anti-AD multitarget-directed drugs. It showed the lowest IC_{50} value against hAChE reported for a peptide (0.99±0.02μM) and inhibited 94.2%±1.2 of AChE-induced Aβ aggregation at 10μM. Furthermore, it inhibited hBChE (IC_{50}, 15.44±0.91μM), showed no *in vivo* toxicity in brine shrimp and had shown moderated radical scavenging and Fe^{2+} chelating capabilities in previous studies. The results are in line with multiple reports showing the utility of the indole moiety for the development of cholinesterase inhibitors.

Introduction

Alzheimer's disease (AD) accounts for 60% to 80% of all dementia cases, a disease that affects more than 55 million people worldwide. With more than 10 million incident cases every year,[1] AD is fatal, progressive and still incurable; causing patients to suffer years of loss of vital neurological functions and their families to face great emotional and financial hardship. It is now widely recognized that the nature of AD is multifactorial.[2] AD patients suffer from extra and intracellular neurotoxic aggregations of amyloid-β (Aβ) peptide and tau protein, respectively, while their synaptic functions and oxidative balance in the brain are compromised.

Although many experts consider the deposition of Aβ, which forms the so-called senile plaques, to be the trigger for all pathological outcomes of AD (amyloid cascade hypothesis),[3] drugs that act directly by inhibiting its deposition or eliminating its aggregates are not yet used for its treatment. Such drugs that could act as disease-modifying therapies are under active research and development.[4] In 2021, the U.S. Food and Drug Administration (FDA) approved the use of the monoclonal antibody Aducanumab against Aβ under the accelerated approval pathway, but its use remains controversial as the FDA suggested further clinical trials to evaluate its benefits due to the refusal of the European Medicines Agency that led to the withdrawal of the marketing authorization application in Europe.[5] Traditional pharmacological treatment of AD is based on the use of compounds capable of reversibly reducing the activity of the cholinesterase enzymes, acetylcholinesterase (AChE, EC 3.1.1.7) and butyrylcholinesterase (BChE, EC 3.1.1.8). These serine hydrolases are responsible for the breakdown of the neurotransmitter acetylcholine (ACh) into acetate and choline, in people affected by AD they show exacerbated activity leading to a decrease in physiological ACh levels. Treatment with cholinesterase inhibitors (ChEIs) enhances the stimulatory action of ACh found in the central and peripheral nervous system.[6]

The currently approved ChEIs (donepezil, rivastigmine and galantamine) primarily target AChE, the most abundant cholinesterase in the central nervous system, where BChE accounts for 20% of total ACh hydrolysis. Despite this, the discovery of dual inhibitors (acting simultaneously on AChE and BChE) has gained special attention in AD drug research, as BChE activity has been found to increase during AD progression and BChE is highly correlated with abnormal Aβ deposition.[7]

The active site of AChE and BChE consists in a catalytic triad (Ser, His and Glu) placed at the bottom of a gorge. At the entrance of the gorge there are other important regions, including the Peripheral Aromatic Site (PAS) whose function in AChE has been characterized in detail. Via the PAS, AChE exerts a chaperone-like activity that could promote the aggregation of the Aβ peptide that leads to the formation of senile plaques.[8] Therefore, it was proposed that non-competitive or mixed-type inhibitors binding the PAS may simultaneously regulate AChE activity and Aβ deposition. PAS consists of 5 residues (Tyr72, Asp74, Tyr124, Trp286 and Tyr341) in hAChE (human AChE) and two (Tyr332 and Asp70) in hBChE (human BChE), where its function is less understood.

Several dual inhibitors as the approved donepezil have shown the ability to interact with key residues of the PAS.[9]

In addition to anticholinergic and antiamyloidogenic compounds, there are drugs with antioxidant and metal chelating activity that are in phases II or III of AD drug development,[10] as oxidative stress and bioactive metals imbalance are related to the neuropathological manifestations of AD.[11] In the recent years, many compounds possessing more than one of the desired properties were proposed as candidates for AD treatment. The single-molecule multitarget approach appears to be especially beneficial for the treatment of AD.[12]

In a previous work, our group reported the AChE inhibitory activity of a series of new peptide analogs of a natural peptide isolated from the skin of the frog *Boana pulchella*.[13] The best analog (W3) showed an *in vitro* IC_{50} (concentration needed to inhibit 50% of enzymatic activity) of 10.42 μM against eeAChE (*Electrophorus electricus* AChE), the lowest value reported at the moment for a short peptide for that AChE variant. W3 and other derivatives also displayed antioxidant and metal-chelating capabilities and were therefore considered interesting molecules for further studies, since peptides are emerging as an important alternative to small molecules within the drug market, with a current market share of 5%.[14]

The present study extends the evaluation of these peptides by testing their *in vitro* inhibitory effects on the pharmacologically more relevant human isoform of AChE, as well as on hBChE. Moreover, the structure-level interactions of the best candidates were studied to examine the inhibitory mechanism by combining experimental kinetics with computational simulations. Finally, the anti-amyloidogenic activity of the best inhibitor was evaluated by performing an *in vitro* AChE-induced Aβ aggregation assay.

Results and Discussion

Design and synthesis

The design and synthesis of this peptide series were reported in a recent publication.[15] Concisely, 19-mer peptide Hp-1935 from *B. pulchella* was used as the base sequence. We first discovered that the moderate eeAChE inhibitory activity of Hp-1935 was concentrated on 10 amino acids (aa) of the center of the sequence by synthesizing that portion, the peptide named LL.[13] Both the original sequence and LL showed a non-competitive, PAS-targeted inhibition mechanism. To increase LL inhibitory activity, various derivatizations of LL were rationally designed and synthesized by mutating the third Pro and/or the seventh Gly aliphatic residues of LL for aromatic ones. The sequences of LL and the mutants are displayed in Table 1. All peptides were synthesized using FMOC solid-phase synthesis. The best analog (W3) having one Trp substitution (Pro 3 Trp mutation) showed a 30-fold higher AChE inhibitory activity on eeAChE and a better ability to neutralize DPPH radicals (DPPH•).

hAChE and hBChE inhibitory activities

Although eeAChE is very useful in the screening stages of cholinesterase inhibitors discovery and development, due to its low cost and high stability, it is more important to test potential candidates on the human variant. For this reason, we performed an *in vitro* inhibitory assay based on the Ellman's reaction using recombinant expressed hAChE/hBChE (rhAChE/rhBChE). The determined IC_{50} values are displayed in Table 2 and the dose-response curves are in Figure 1A, B.

Table 1. Sequences of the synthetic peptides.

Peptide	Mutation	Sequence	MW (Da)[a]
LL	-	LGPVSKGKLL-NH_2	1010.97
Y3	Pro 3 Tyr	LGYVSKGKLL-NH_2	1077.09
F3	Pro 3 Phe	LGFVSKGKLL-NH_2	1059.68
W3	Pro 3 Trp	LGWVSKGKLL-NH_2	1100.12
W7	Gly 7 Trp	LGPVSKWKLL-NH_2	1138.63
Y3Y7	Pro 3 Tyr/Gly 7 Tyr	LGYVSKYKLL-NH_2	1182.95
Y3W7	Pro 3 Tyr/Gly 7 Trp	LGYVSKWKLL-NH_2	1205.06
W3W7	Pro 3 Trp/Gly 7 Trp	LGWVSKWKLL-NH_2	1229.43
F3 (4-F)	Pro 3 4-F Phe	LG(4-Fluoro)FVSKWKLL-NH_2	1079.18

[a] Sanchis et al. (2022). All peptides are amidated at their C-terminus. Final purity > 90%

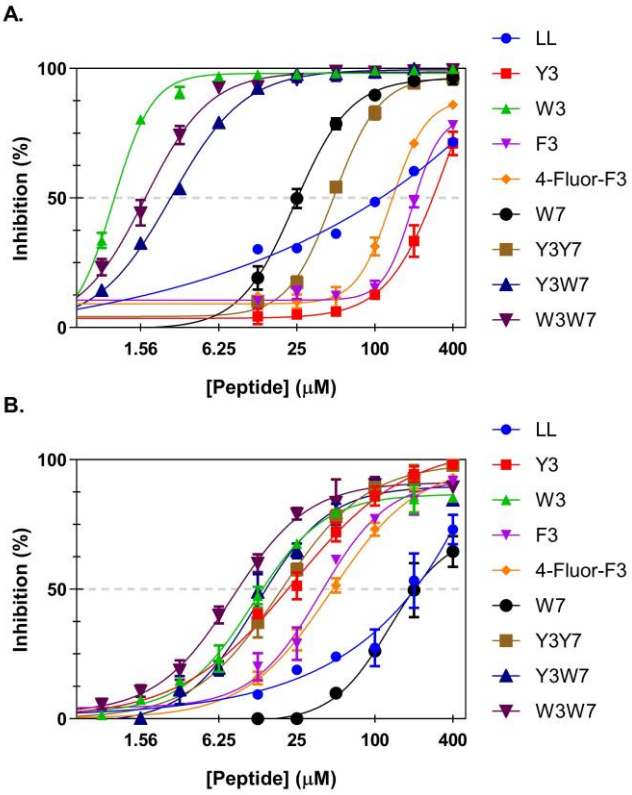

Figure 1. Percentage inhibition of (A) hAChE and (B) hBChE activity by LL and derivatives vs. peptide concentration (logarithm scale). Points express the mean ± SEM (n = 3).

As with eeAChE, the most active peptide on rhAChE was W3, but in this case its activity was 10-fold higher with an IC_{50} of 0.99

± 0.02 µM. A higher activity against rhAChE was expected, as the human variant is normally more sensitive to inhibitors than the *E. electricus* variant.[16] To our knowledge, there are no reports of a more potent short peptide inhibitor of hAChE. To date, the most active one was the *de novo*-designed octapeptide OP5 reported by Mondal et al. (2018) (IC_{50}, 7.34 µM).[17] Remarkably, W3 peptide also showed significant inhibitory activity on rhBChE (IC_{50}, 15.44 ± 0.91 µM). Furthermore, moderated DPPH• scavenging, metal chelating activities, and low hemolysis evaluated in human erythrocytes were previously reported for this peptide.[15]

The inhibition results of the other derivatives revealed that the peptide W3W7 with two Trp substitutions inhibited hAChE and hBChE with IC_{50} values of 1.70 ± 0.05 µM and 9.40 ± 0.48 µM, respectively. This peptide had shown the highest anti-DPPH• activity and here was the most potent against hBChE. No reports of a most active hBChE peptide inhibitor were found. The IC_{50} values from the other derivatives ranged from 2.66 ± 0.05 µM to 267.30 ± 10.21 µM for AChE inhibitors and 16.16 ± 1.04 µM to 255.60 ± 17.50 µM for BChE inhibitors, pointing to a general positive effect of the aromatic substitution strategy to increase the inhibitory activity of LL.

Kinetics and inhibitory mechanism of the best derivatives on hAChE and hBChE

Previous kinetics and computational studies had demonstrated that the inhibitory mechanism of the original peptide Hp-1935 and its derivatives is of reversible non-competitive type acting in the PAS. Herein, we studied the interactions of W3 on hAChE and W3W7 on hBChE at an atomistic level *in silico*.[13,15] We also performed kinetic measurements of the reaction of the best inhibitor to calculate its inhibitory constant (K_i). Computational experiments included the molecular modeling of the peptide structures in water, flexible docking calculations for the peptide-enzyme complexes followed by 100 ns of molecular dynamics (MD) simulations to assess the reliability of the docking results, and an energetic Molecular Mechanics-Generalized Born Surface Area (MM/GBSA) analysis for an in-depth view of the interaction mechanism.

The K_i of the best inhibitor on hAChE was 1.61 ± 0.47 µM. As expected from previous results, Michaelis-Menten curves indicate a non-competitive inhibitory mechanism (Supporting Information Figure S1). The docking calculations for W3 with hAChE and W3W7 with hBChE placed the peptides on the PAS. MD simulations corroborated these predictions, as the configuration was maintained with only slight rearrangements during the production runs. Close-up views of representative snapshots from the last 10 ns of simulations are shown in Figures 2A and 2B for hAChE-W3 and hBChE-W3W7 respective complexes.

The Pro 3 Trp mutation allowed the formation of aromatic-aromatic interactions between the indole side chain of the incorporated Trp residue (Trp3) and residues of the PAS. The large aromatic pocket was a better fit for the introduced Trp than for the original Pro. At the PAS core, AChE_Trp286 plays a critical role in accommodating the cationic substrate ACh in the early stages of substrate-AChE interactions.[18] In Figure 2A it can be observed that W3_Trp3 is positioned close to AChE_Trp286 forming an aromatic parallel-displaced π–π stacking interaction that was maintained throughout the simulation (Supporting Information Figure S4). Moreover, the results suggest that an additional T-shaped aromatic interaction with AChE_Tyr337 of the anionic subsite stabilizes the final orientation of W3_Trp3. The anionic subsite is a choline-binding pocket that interacts with the charged quaternary amine of ACh and is the binding site of important hAChE inhibitors such as tacrine.[19,20] These interactions can be considered to account for the much higher inhibitory activity of the W3 derivative when compared to LL.

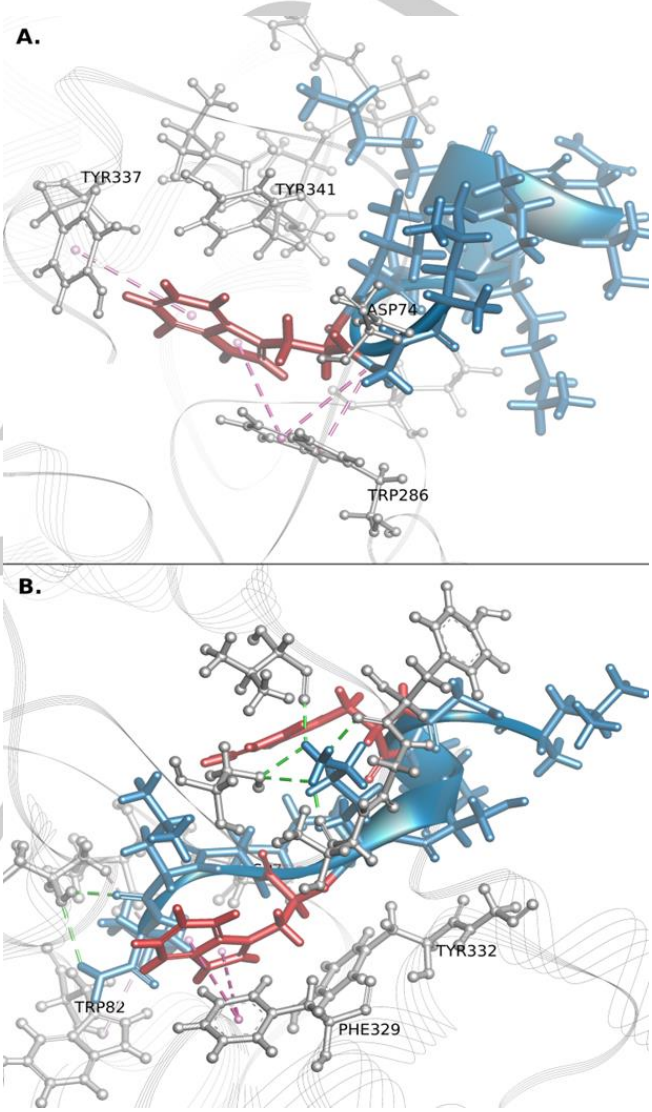

Figure 2. Close-up view of the predicted binding pose for (A) W3 peptide on hAChE and (B) W3W7 peptide on hBChE. Enzymes are displayed in grey, ligands in blue, and the mutated residues in red. Processed with DS Visualizer program (BIOVIA).

The MM/GBSA calculation provides valuable data on the atomistic enzyme-ligand interactions, as it is calculated as an average of 100 structures from the last 10 ns of simulation and quantifies the binding affinity. The calculated binding affinities for the W3-hAChE and W3W7-hBChE systems were -24.77 ± 7.44 kcal/mol and -24.31 ± 3.77 kcal/mol, respectively. The energy decomposition

Table 2. Cholinesterase inhibitory potencies and radical-scavenging activities (DPPH assay) of peptide LL and its analogs.

Peptide[a]	rhAChE IC_{50} (μM)	rhBChE IC_{50} (μM) [b]	eeAChE IC_{50} (μM)[a]	$DPPH^{\bullet}$ EC_{50} (μM)[a,b]
LL	97.89 ± 7.13	192.20 ± 22.03	317.90 ± 28.78	-
Y3	267.30 ± 10.21	23.27 ± 1.08	-	-
F3	208.20 ± 14.50	49.89 ± 3.52	-	-
W3	0.99 ± 0.02	15.44 ± 0.91	10.42 ± 1.02	78.31 ± 18.18
W7	25.77 ± 0.77	255.60 ± 17.50	299.50 ± 37.69	66.94 ± 14.34
Y3Y7	50.67 ± 2.09	19.11 ± 0.72	320.80 ± 17.69	-
Y3W7	2.66 ± 0.05	16.16 ± 1.04	85.91 ± 4.13	43.94 ± 8.12
W3W7	1.70 ± 0.05	9.40 ± 0.48	56.63 ± 3.06	27.58 ± 8.74
F3 (4-F)	137.90 ± 7.81	47.18 ± 1.44	-	-
Rivastigmine	23.30 ± 0.44	0.08 ± 0.04	34.17 ± 6.00	-

[a] Sanchis et al. (2022). [b] EC_{50} express the peptide concentration that causes a 50% decrease in the $DPPH^{\bullet}$ absorbance. Data express as mean ± SEM (n = 3)

analysis results are consistent with the binding mode results. The per-residue free energy decomposition by ligand residue shows that W3_Trp3 contributes for the highest affinity (lower binding free energy) to the stabilization of the complex (Figure 3A). Moreover, the ΔG decomposition by receptor residue shows that AChE_Asp74, AChE_Trp286, and AChE_Tyr341 residues bind with the highest affinity to the peptide (Figure 3B), which confirms that the PAS is the main binding region.

The analysis of the predicted conformation of the W3W7-hBChE complex also reveals the important role of the incorporated Trp residues for enzyme-ligand affinity. In this case, the replacement of Gly 7 by Trp appears to be critical as the indole group of W3W7_Trp7 is well accommodated on the PAS and close to the anionic site via T-shaped aromatic interactions between this fragment and BChE_Tyr332 of the PAS and BChE_Phe329 of the anionic site (Figure 2B). This conformation could explain the hBChE inhibitory activity of the W3W7 derivative, as interactions with BChE_Phe329 and BChE_Tyr332 have been observed in other hBChE inhibitors.[21,22] Both aryl residues (Phe329 and Tyr332) are critical for hBChE activity, as they have been implicated in substrate binding in a site competition study of wild-type and mutant BChE with different substrates.[23,24] Another interaction that can contribute to the inhibitory activity of W3W7 is observed between W3W7_Leu10 and BChE_Trp82 of the enzymatic choline-binding pocket. These predictions were confirmed by the energy per-residue decomposition that estimated binding free energies of -6.76 kcal/mol and -6.11 kcal/mol for residues W3W7_Trp7 and W3W7_Leu10 and -2.00 kcal/mol, -2.22 kcal/mol and -4.52 kcal/mol for residues W3W7_Asp70, W3W7_Trp82 and W3W7_Tyr332, respectively (Figure 3A, B). Furthermore, the results of these calculations suggest that the replacement of Pro 3 by Trp was also important for the binding of W3W7 with BChE (ΔG, -6.16 kcal/mol).

The fact that the addition of an indole moiety increased the inhibitory activity is not surprising. Many researchers have exploited this chemical group in search of new cholinesterase inhibitors as single or multifunctional ligands. Meden et al. successfully designed and synthesized a series of *in vivo* active Trp-derived BChE inhibitors.[25] The crystal structure of their best compound with hBChE revealed the critical role of the inhibitor indole ring within the acyl-binding pocket of hBChE. Shan et al. found that the indole fragment was important for the retention of bioactivity when studying a series of alkaloids.[26] Nadeem et al. used the indole group to enhance the interactions with target hydrophobic residues in a series of mono- and bi-indole derivatives.[22] They discovered nanomolar inhibitors showing stabilizing contacts between the indole rings of the ligands and residues Trp286 and Tyr341 for AChE and Tyr332 for BChE. Similar findings were also achieved by other authors.[27-31]

In vitro AChE-induced Aβ aggregation assay

AChE inhibitors selectively binding to the PAS such as propidium iodide (PI) can interfere with the AChE-catalyzed Aβ aggregation process.[32,33] This can be explained by the accumulation of evidence showing that the PAS can bind to Aβ, promoting the formation of Aβ fibrils.[34]

To evaluate the anti-aggregation ability of the most active derivative (W3) we performed an *in vitro* fluorometric Thioflavin T aggregation assay following the method of Chen et al. based on the monitoring of the changes in the ThT fluorescence intensity,[35] which depends on the presence of aggregated Aβ constructs, in the presence of AChE and the presence or absence of 10 μM of W3 at different times. PI was used as a positive control. W3 at 10 μM showed a strong ability to inhibit AChE-induced Aβ aggregation, as can be seen in Figure 4. The fluorescence was measured after 3, 5 and 8 hours of aggregation. After 8 hours, the percentage inhibition displayed by W3 was 94.2 % ± 1.2.

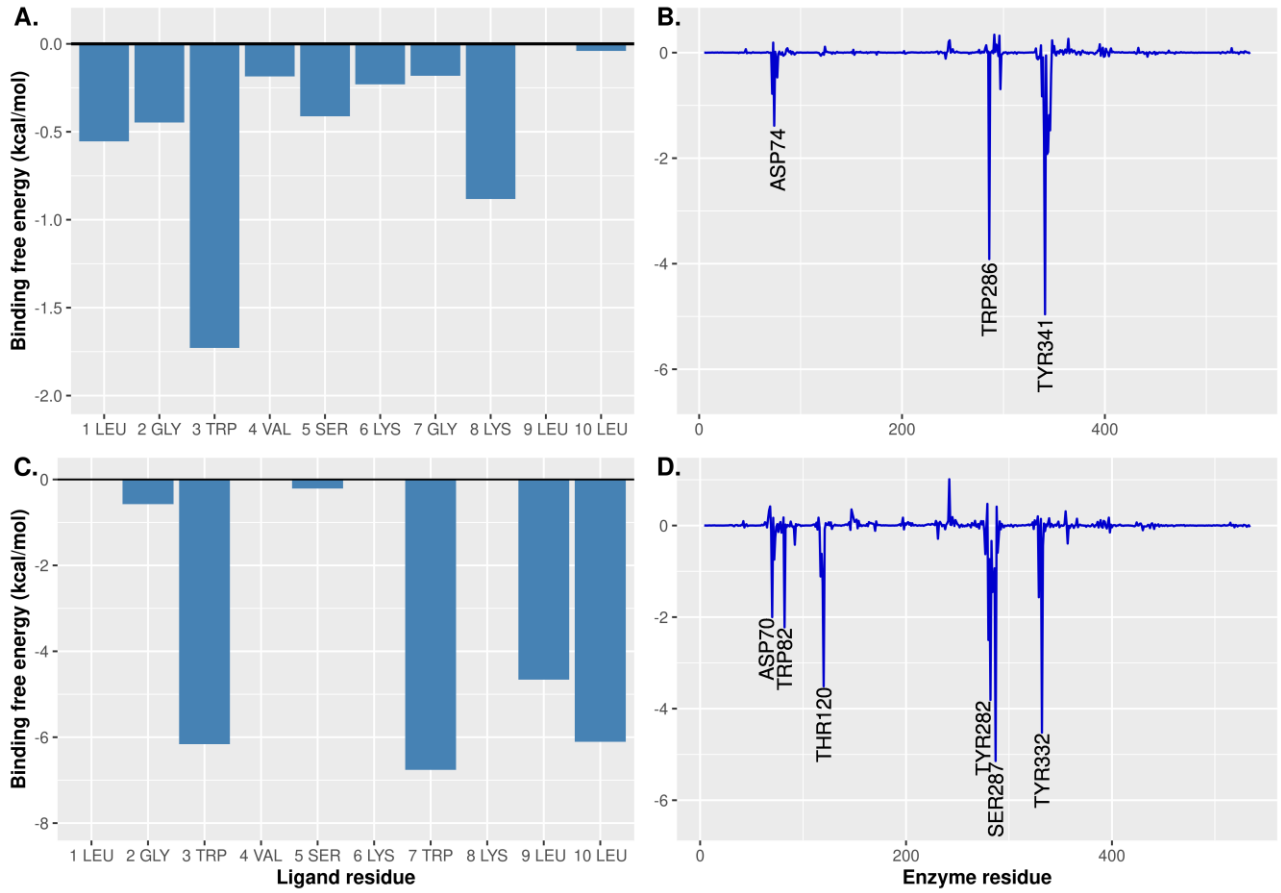

Figure 3. Ligand−residue interaction energies from MM/GBSA free binding energy decomposition for (A) W3-hAChE by ligand residue (B) W3-hAChE by receptor residue (C) W3W7-hBChE by ligand residue (D) W3W7-hBChE by receptor residue.

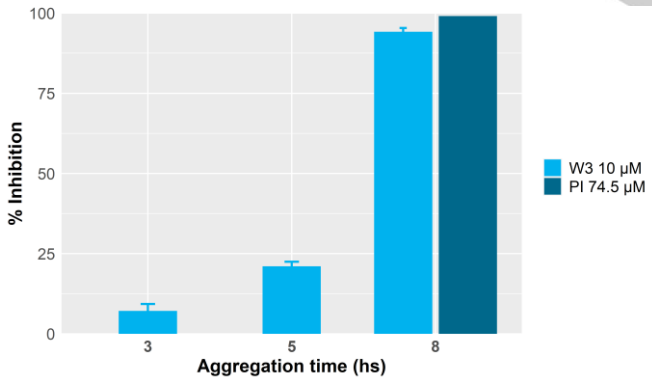

Figure 4. AChE-induced Aβ aggregation inhibition by W3 derivative after 3, 5 and 8 hours of reaction. The bars express the mean ± SEM (n = 3).

This inhibitory activity can be justified by the predicted interaction of W3 with key residues of the PAS as the Trp residue at its center.[15] Many reported anti-aggregation compounds showed interactions with this residue.[35-37] Despite this, we must consider that a direct W3-Aβ interaction may be contributing to the inhibition, as reported for other peptides or mini-proteins. Murray et al. designed a mini-protein that inhibited Aβ aggregation through protein-protein interactions.[38] Similarly, Preetham et al. developed a β-aminopyrrolidine containing 12-mer peptides derived from the Aβ sequence displaying a potent antiaggregant activity.[39] No reports of peptides selectively inhibiting AChE-induced Aβ aggregation were found in the literature.

In vivo toxicity in *Artemia salina* (*A. salina*)

To get a comprehensive analysis of the toxic profiles induced by the best inhibitors, W3 and W3W7, toxicity was tested in brine shrimp (*A. salina*) larvae. The results are shown in Figure 5. The brine shrimp lethality assay had shown a strong correlation with the standard toxicity MTT assay and has been proposed as a good alternative to evaluate the toxicity of small compounds.[40] The results showed no toxic effects for W3 and W3W7 derivatives at the tested concentrations (12.5 – 100 µM) as no difference with the negative control (saline solution) was observed. These results are in good agreement with the previously tested hemolytic activity which was low.[15] In particular, W3 was hemolytic at concentrations much greater than the concentrations needed to achieve 50% inhibition of hAChE and its LD_{50} (concentration which causes the death of 50 %) on *A. salina* larvae was >100 µM.

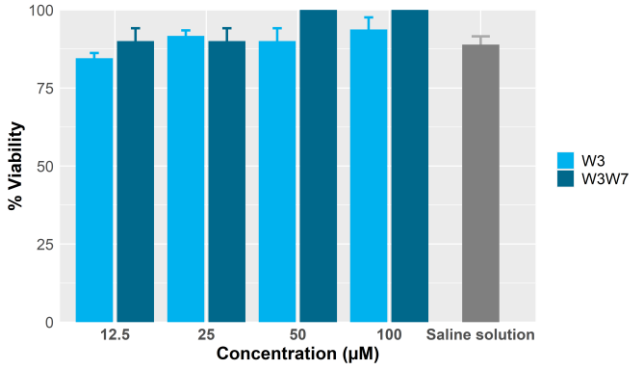

Figure 5. Toxic effect of the best inhibitors in brine shrimp. Percentage of Artemia nauplii viability vs. peptide concentration. A saline solution was used as a positive control. The bars express the mean ± SEM (n = 3).

Conclusion

This study reports the *in vitro* inhibitory activity on the human cholinesterases of a series of peptide derivatives of a natural sequence isolated from the frog *B. pulchella* and the AChE-induced Aβ anti-aggregation activity of the best inhibitor. We found that mutation of one or two aliphatic residues of the original sequence by Trp residues notably increased the inhibitory activity. The most active compound W3 showed an IC_{50} value of 0.99 ± 0.02 μM against hAChE, a 100-fold higher value than that of the base sequence (97.89 ± 7.13 μM). Additionally, W3 inhibited hBChE (IC_{50}, 15.44 ± 0.91 μM) and showed a percentage inhibition of 94.2 % ± 1.2 against AChE-induced Aβ aggregation. This peptide had also shown moderated radical scavenging and Fe^{2+} chelating capabilities, low hemolysis, and low *in vivo* toxicity in brine shrimp. Peptides are attracting great attention as therapeutic drugs for their unique properties. Considering the multifunctional profile showed by the W3 peptide, we propose it as an interesting scaffold for further development of a multitarget-directed drug against AD.

Experimental Section

Chemistry. Peptides were synthesized through FMOC solid-phase peptide synthesis (SPPS) using a Rink SS 1% DVB resin (Advanced Chemtech, USA). All the other chemicals and reagents were purchased from Merck Sigma-Aldrich (Merck KGaA, Germany). α-amine was deprotected with piperidine at 20% in N,N-dimethylformamide (DMF) (three times 1 min). Carbonyl activation and 1 h couplings were realized using 2-(1H-Benzotriazole-1-yl)-1,1,3,3-tetramethylammonium tetrafluoroborate (TBTU), 1-hydroxybenzotriazole hydrate (HOBt) and diisopropylethylamine (DIEA). Peptides were separated from the resin with a TFA/H2O/TIS (95:2.5:2.5) mixture for 2.5 h and washed with several cycles of precipitation with cold ether and centrifugation. Samples were purified and further analyzed by RP-HPLC using an Atlantis (Waters) C18 column (5 μm, 4.6 mm×150 mm) with a linear gradient of ACN/H2O (flow rate 0.8 ml/min) for 25 min in a Waters HPLC System; TFA 0.1% was added to each solvent. Peptides were analyzed by MALDI-MS in a MALDI-TOF-TOF Abi Sciex 4800 (Pasteur Institute, Montevideo, Uruguay). The observed masses were in full agreement with the calculated masses. Aβ peptide (1–40) was synthesized by following the same procedure with the H-Rink amide ChemMatrix resin purchased from Sigma-Aldrich (Merck KGaA, Germany).

Cholinesterases preparation. Recombinant hAChE was produced and purified as previously described.[41] Briefly, the recombinant hAChE was expressed using Chinese Hamster Ovary cells (CHO). The secreted enzyme was recovered from the culture medium and purified by affinity liquid chromatography (HisTrap, monoQ, Cytiva, France) followed by gel filtration (Superdex 200, Cytiva, France). The recombinant enzyme was then concentrated, flash frozened in liquid nitrogen and stored at -80°C. Recombinant hBChE, was produced and purified as previously described.[25] Briefly, the recombinant hBChE was secreted out of CHO cells and the protein was purified from the culture medium following a two-steps protocol using both BChE-specific affinity chromatography (Hupresin®, Chemforase, France) followed by gel filtration (Superdex 200, Cytiva, France).

Cholinesterase inhibitory assay. The *in vitro* inhibitory activity of the peptides was evaluated by following a previously reported method based on Ellman's colorimetric assay.[15,42] The reaction was performed in a final volume of 100 μL with 100 pM or 1 nM rhAChE or rhBChE, respectively, 0.4 mM acetylthiocholine iodide (ATCI, Sigma-Aldrich) or s-butyrylthiocholine iodide (BTCI, Sigma-Aldrich), 0.33 mM 5,5-dithiobis-(2-nitrobenzoic acid) (DTNB, Sigma-Aldrich) and the peptide at 400-0.78 μM, in 0.1 M phosphate buffer (pH = 8.0). The enzyme and peptide solutions were mixed and incubated for 15 min (room temperature) and the reaction was started by the addition of the substrate and DTNB solutions. Absorbance at 405 nm was measured after 5 min in a 96-well microplate reader (Thermo Fisher FC Multiskan). Percentage inhibition (I%) was calculated as 100 * (Ai-Ab) / (A0-Ab) where Ai is the absorbance of the solution containing the sample, Ab is the absorbance of the blank (no enzyme, no inhibitor) and A0 is the absorbance of the control (no inhibitor). Enzyme residual activity percentage (equal to 100 - I%) values were used to calculate the IC_{50} values with a four-parameter logistic curve estimated using R v. 4.0.4. Rivastigmine was used as a positive control. Kinetic measurements were realized by monitoring the absorbance for 5 min every 3 s, under the same conditions at the different substrate and peptide concentrations (0 – 0.5 mM). The initial velocities (v_0) in the presence and absence of the tested peptides were calculated. K_i values were calculated using the Michaelis–Menten (MM) equations for non-competitive inhibitors according to Copeland.[43] At least three independent experiments were performed.

Molecular modeling and flexible docking. The 3D structures of the peptides were modeled *de novo* using PEPFOLD 3.5 algorithm on the RPBS Mobyle portal.[44,45] The best models were optimized by performing 400 ns of MD simulations in explicit TIP3P water with the same conditions used for the enzyme-peptides complexes (see below). The models were docked with Protein Data Bank entries 4EY7 (hAChE) or 2PM8 (hBChE) previously prepared by adding missing residues with Modeller 10.3,[46] removing all ligands, water molecules and ions. HADDOCK2.4 program was used to execute the semi-flexible docking calculations with default docking parameters for protein-protein docking. All ligand residues and all active residues of hAChE and hBChE were marked as active (flexible) residues.[47,48] The calculations were run on the HADDOCK Web Server. The best-scored structures according to the HADDOCK score function were promoted to MD simulations.

MD simulations. All-atom MD simulations were performed with the Amber 18.0 package.[49] Topology and initial coordinate files were produced with the tLEaP module.[50] The best models from the docking studies were applied with ff14SB force-field and solvated with a cubic periodic box with a margin distance of 12 Å containing TIP3P water molecules and neutralizing counter ions. The pre-production preparation of the structures by performing a two-step energy minimization process, a thermalization, and 200 ps of equilibration to adjust system density. The 100 ns production was performed using the NPT ensemble under a target temperature of 298 K and target pressure of 1 atm with the GPU implementation of the PMEMD program and trajectory snapshots were saved every 1 ps. Newton motion equations were integrated using a 2 fs timestep.[51,52] Finally, the CPPTRAJ module was used to calculate the

Root-mean-square deviation of atomic positions (RMSD) of the peptide-protein complex during the simulations and to perform a k-means clustering with the calculated structures (k = 10). A representative snapshot was then obtained by extracting the structure with the lowest cumulative distance to every other point of the most populated cluster.

MM/GBSA calculations. A MM/GBSA per-residue free energy decomposition analysis was performed to provide insight into the interaction energies for each residue of the predicted complexes.[53-55] The calculations were executed by using the MMPBSA.py script of the Amber 18.0 package and taking 100 frames from the last 10 ns of the simulation. Entropies were not included in the calculation. The inclusion of an entropic term is simply neglected by many applications due to the extremely expensive computational cost and relatively low prediction accuracy.[56] For this reason, new alternatives for the estimation of the theoretical entropy are being investigated.[57]

AChE-Induced β-Amyloid Aggregation Testing. The AChE-induced Aβ aggregation inhibitory activity of the most active derivative was tested *in vitro* as described by Chen et al.[35] First, a 20 mg/ml solution of the synthesized Aβ peptide in hexafluoroisopropanol (HFIP) was prepared. The solvent was evaporated with a nitrogen stream and dried under a high vacuum for 2 hs. Then, a 2 mM Aβ peptide stock solution was prepared and stored at -20°C by dissolving the residue in dimethyl sulfoxide (DMSO). The aggregation reaction was carried out by incubating 100 µM Aβ peptide (5 µL) and 1 U/mL eeAChE (40 µL) (E.C. 3.1.1.7, type VI-S from the electric eel, Sigma-Aldrich) in a 100 µl final volume in the presence and absence of 10 µM W3 derivative, during 3, 5 and 8 hours at 25 °C. The solution buffer was 25 mM NaH_2PO_4 and 100 mM NaCl (pH = 8.0). At each specific spot time, a thioflavin T solution (Sigma-Aldrich, final concentration 2.5 µM) was added and the fluorescence was monitored at 450 nm (λexc) and 482 nm (λem) with excitation and emission slits of 2 nm bandwidth with a Perkin Elmer LS55 fluorescence spectrophotometer. The fluorescence emission spectrum was recorded between 450 and 600 nm with excitation at 446 nm. The background fluorescence from 2.5 µM thioflavin T and AChE was removed. The percent inhibition was calculated as 100 - (IFi - IFo /100) where IFi and IF0 are the fluorescence intensities obtained for the Aβ peptide and eeAChE solution in the presence and absence of inhibitor, respectively. 74.5 µM propidium iodide was used as the positive control. The sample was tested in triplicate.

Brine shrimp (*A. salina*) bioassay. Sea water was prepared following formulations and conditions from the maritime ordinance previously described.[55] 100 mL of seawater previously oxygenated to achieve an oxygen saturation of 90 % was placed in graduated cylinders with aeration. Then, 100 mg of *A. salina* cysts were added and incubated in the presence of visible light (750 lm), at 25 ± 1 °C for 48 hs. After that, aeration was stopped. The hatched Brine shrimp (nauplii), which remained in the middle section of the graduated cylinder, were collected. The toxic activity of W3 and W3W7 in *A. salina* was evaluated according to previous methods with slight modifications.[40,59,60] Following the addition of 360 µL of 100, 50, 25, and 12.5 µM peptide solutions, 6 nauplii were placed in each well of the 96-well microtiter plates. The incubation was performed at 25 °C in the absence of light for 24 h. The dead nauplii were counted under a stereoscopic microscope, and the percentage of mortality at each concentration was calculated as (Ms/N) x 100 where Ms is the number of dead individuals in the sample analyzed and N is the total number of exposed individuals. LD_{50} was calculated using the R package BioRssay, based on probit functions.[61] Assays were performed in triplicate, with two positive controls (larvae in methanol 99,9% and larvae in a 408 µM K_2Cr2O_7 aqueous solution) for 100 % mortality and a negative control (saline solution).

Acknowledgements

JD and XB were supported by the French Ministry of Armed Forces (Direction Générale de l'Armement and Service de Santé des Armées) under grant number NBC-5-C-4210.

Keywords: Alzheimer's disease • cholinesterase inhibitors • amyloid beta-peptides • peptides

[1] WHO, *Dementia*, September 2022, World Health Organization, https://www.who.int/news-room/fact-sheets/detail/dementia

[2] S. O. Bachurin, G. F. Makhaeva, E. F. Shevtsova, N. P. Boltneva, N. V. Kovaleva, S. V. Lushchekina, E. V. Rudakova, L. G. Dubova, D. V. Vinogradova, V. B. Sokolov, A. Y. Aksinenko, V. P. Fisenko, R. J. Richardson, G. Aliev, *Sci. Rep*. **2019**, *9*, 4873.

[3] H. Hampel, J. Hardy, K. Blennow, C. Chen, G. Perry, S. H. Kim, V. L. Villemagne, P. Aisen, M. Vendruscolo, T. Iwatsubo, C. L. Masters, M. Cho, L. Lannfelt, J. L. Cummings, A. Vergallo, *Mol. Psychiatry* **2021**, *26*, 5481-5503.

[4] C. Song, J. Shi, P. Zhang, Y. Zhang, J. Xu, L. Zhao, R. Zhang, H. Wang, H. Chen. *Transl. Neurodegener.* **2022**, *11*, 18.

[5] S. Liu, M. Fan, J Xu, L. Yang, C. Qi, Q. Xia, J. Ge, *J Neuroinflammation* **2022**, *19*, 35.

[6] G. Marucci, M. Buccioni, D. Dal Ben, C. Lambertucci, R. Volpini, F. Amenta, *Neuropharmacology* **2021**, *190*, 10835.

[7] S. Zhou, G. Huang, *Biomed. Pharmacother*. **2022**, *146*, 112556.

[8] M. Pohanka, *Biomed. Pap. Med. Fac. Univ. Palacky. Olomouc. Czech. Repub*. **2011**, *155*, 219-229.

[9] Y. Pourshojaei. *Sci. Rep*. **2019**, *9*, 19855.

[10] J. Cummings, G. Lee, K. Zhong, J. Fonseca, K. Taghva, *Alzheimers. Dement. (N Y)* **2021**, *7*, e12179.

[11] M. Taheri, S. Aslani, H. Ghafouri, A. Mohammadi, V. A. Moghaddam, N. Moradi, H. Naeimi, *BMC Chem*. **2022**, *16*, 7.

[12] O. Benek, J. Korabecny, O. Soukup, *Trends Pharmacol. Sci*. **2020**, *41*, 434-445.

[13] I. Sanchis, R. Spinelli, N. Aschemacher, M. V. Humpola, A. Siano, *Amino Acids* **2020**, *52*, 387-396.

[14] M. Muttenthaler, G. F. King, D. J. Adams, P. F. Alewood, *Nat. Rev. Drug. Discov*. **2021**, *20*, 309-325.

[15] I. Sanchis, R. Spinelli, N. Aschemacher, A. S. Siano *Amino Acids* **2022**, *54*, 181-192.

[16] V. Sepsova, J. Z. Karasova, J. Korabecny, R. Dolezal, F. Zemek, B. J. Bennion, K. Kuca, *Int J Mol Sci*. **2013**, *14*, 16882-900.

[17] P. Mondal, V. Gupta, G. Das, K. Pradha, J. Khan, P. K. Gharai, S. Ghosh *ACS Chem. Neurosci*. **2018**, *9*, 2838-2848.

[18] G. Johnson, S. W. Moore *Curr. Pharm. Des*. **2006**, *12*, 217-225.

[19] K. V. Dileep, K. Ihara, C. Mishima-Tsumagari, M. Kukimoto-Niino, M. Yonemochi, K. Hanada, M. Shirouzu, K. Y. J. Zhang, *Int. J. Biol. Macromol*. **2022**, *210*, 172-181.

[20] K. B. Karunakaran, A. Thiyagaraj, K. Santhakumar, *Nat Prod Bioprospect*. **2022**, *12*, 6.

[21] D. Vicente-Zurdo, N. Rosales-Conrado, M. E. León-González, L. Brunetti, L. Piemontese, A. R. Pereira-Santos, S. M. Cardoso, Y. Madrid, S. Chaves, M. A. Santos, *Biomedicines* **2022**, *10*, 1510.

[22] M. S. Nadeem, J. A. Khan, I. Kazmi, U. Rashid, *ACS Omega* **2022**, *7*, 9369-9379.

[23] T. L. Rosenberry, X. Brazzolotto, I. R. Macdonald, M. Wandhammer, M. Trovaslet-Leroy, S. Darvesh, F. Nachon, *Molecules* **2017**, *22*, 2098.

[24] I. R. Macdonald, *Biochemistry* **2012**, *51*, 7046-53.

[25] A. Meden, D. Knez, M. Jukič, X. Brazzolotto, M. Gršič, A. Pišlar, A. Zahirović, J. Kos, F. Nachon, J. Svete, S. Gobec, U. Grošelj, *Chem. Commun. (Camb)* **2019**, *55*, 3765-3768.

[26] Z. Zhan, Q. Yu, Z. Wang, W. Shan, *Bioorg. Med. Chem. Lett*. **2010**, *20*, 6185-7.

[27] M. M. Ismail, M. M. Kamel, L. W. Mohamed, S. I. Faggal, *Molecules* **2012**, *17*, 4811-23.

[28] M. Fadaeinasab, A. Basiri, Y. Kia, H. Karimian, H. M. Ali, V. Murugaiyah, *Cell. Physiol. Biochem*. **2015**, *37*, 1997-2011.

[29] G. Zhan, R. Miao, F. Zhang, G. Chang, L. Zhang, X. Zhang, H. Zhang, Z. Guo, *Bioorg. Chem*. **2020**, *102*, 104136.

[30] T. Padrtová, P. Marvanová, R. Kubínová, J. Csöllei, O. Farsa, T. Goněc, K. Odehnalová, R. Opatřilová, J. Pazourek, A. Sychrová, K. Šmejkal, P. Mokrý, *Curr. Org. Synth*. **2020**, *17*, 576-587.
[31] T. Wichur, A. Pasieka, J. Godyń, D. Panek, I. Góral, G. Latacz, E. Honkisz-Orzechowska, A. Bucki, A. Siwek, M. Głuch-Lutwin, D. Knez, X. Brazzolotto, S. Gobec, M. Kołaczkowski, R. Sabate, B. Malawska, A. Więckowska, *Eur. J. Med. Chem*. **2021**, *225*, 113783.
[32] M. Bartolini, C. Bertucci, V. Cavrini, V. Andrisano, *Biochem. Pharmacol*. **2003**, *65*, 407-16.
[33] J. Alarcón-Enos, E. Muñoz-Núñez, M. Gutiérrez, S. Quiroz-Carreño, E. Pastene-Navarrete, C. Céspedes Acuña. *J. Enzyme Inhib. Med. Chem*. **2022**, *37*, 1845-1856.
[34] Z. Sang, P. Bai, Y. Ban, K. Wang, A. Wu, J. Mi, J. Hu, R. Xu, G. Zhu, J. Wang, J. Zhang, C. Wang, Z. Tan. L. Tang, *Bioorg. Chem*. **2022**, *127*, 106007.
[35] X. Chen, S. Wehle, N. Kuzmanovic, B. Merget, U. Holzgrabe, B. König, C. A. Sotriffer, M. Decker, *ACS Chem. Neurosci*. **2014**, *5*, 377-89.
[36] E. Viayna, R. Sabate, D. Muñoz-Torrero. *Curr. Top. Med. Chem*. **2013**, *13*, 1820-42.
[37] D. Malafaia, A. Oliveira, P. A. Fernandes, M. Jramos, H. M. T. Albuquerque, A. M. S. Silva, *Int. J. Mol. Sci*. **2021**, *22*, 4145.
[38] K. A. Murray, C. J. Hu, S. L. Griner, H. Pan, J. T. Bowler, R. Abskharon, G. M. Rosenberg, X. Cheng, P. M. Seidler, D. S. Eisenberg, *Proc. Natl. Acad. Sci. U S A* **2022,** *119*, e2206240119.
[39] H. D. Preetham, U. Muddegowda, K. S. Sharath Kumar, S. Rangappa, K. S. Rangappa, *J. Pept. Sci*. **2022**, *28*, e3386.
[40] S. Rajabi, *Daru*, **2015**, *23*, 20.
[41] I. Zueva, J. Dias, S. Lushchekina, V. Semenov, M. Mukhamedyarov, T. Pashirova, L. Nurullin, *Neuropharmacology* **2019**, *155*, 131-141.
[42] G. L. Ellman, K. D. Courtney, V. Andres Jr, R. M. Feather-Stone. *Biochem. Pharmacol*. **1961**, *7*, 88-95.
[43] R. A. Copeland, *Methods Biochem. Anal*. **2005**, *46*, 1-265.
[44] Y. Shen, J. Maupetit, P. Derreumaux, P. Tufféry, *J. Chem. Theor. Comput*. **2014**, *10*, 4745-4758.
[45] P. Thévenet, Y. Shen, J. Maupetit, F. Guyon, P. Derreumaux, P. Tufféry, *Nucleic Acids Res*. **2012**, *40*, 288-293.
[46] A. Sali, T. L. Blundell, *J. Mol. Biol*. **1993**, *234*, 779-815.
[47] C. Dominguez, R. Boelens, A. M. Bonvin, *J Am Chem Soc*. **2003**, *125*, 1731-1737.
[48] G. C. P. van Zundert, J. P. G. L. M. Rodrigues, M. Trellet, C. Schmitz, P. L. Kastritis, E. Karaca, A. S. J. Melquiond, M. van Dijk, S. J. de Vries, A. M. J. J. Bonvin, *J. Mol. Biol*. **2016**, *428*, 720-725.
[49] D. A. Case, T. E. Cheatham, T. Darden, H. Gohlke, R. Luo, K. M. Jr. Merz, A. Onufriev, C. Simmerling, B. Wang, R. Woods, *J. Computat. Chem*. **2005**, *26*, 1668–1688.
[50] J. A. Maier, C. Martinez, K. Kasavajhala, L. Wickstrom, K. E. Hauser, C. Simmerling, *J. Chem. Theory Comput.* **2015**, *11*, 3696–3713.
[51] A. W. Götz, M. J. Williamson, D. Xu, D. Poole, S. Le Grand, R.C. Walker, *J. Chem. Theory Comput*. **2012**, *8*, 1542–1555.
[52] R. Salomon-Ferrer, A. W. Götz, D. Poole, S. Le Grand, R. C. Walker, *J. Chem. Theory Comput*. **2013**, *9*, 3878–3888.
[53] V. Tsui, D. A. Case, *Biopolymers* **2000**, *56*, 275-291.
[54] G. Rastelli, A. Del Rio, G. Degliesposti, M. Sgobba, *J. Comput. Chem*. **2010**, *31*, 797-810.
[55] V. Zoete, M. B. Irving, O. Michielin, *J. Mol. Recognit.* **2010**, *23*, 142-152.
[56] H. Sun, L. Duan, F. Chen, H. Liu, Z. Wang, P. Pan, F. Zhu, J. Z. H. Zhang, T. Hou, *Phys. Chem. Chem. Phys*. **2018,** *20*, 14450-14460.
[57] S. Wan, A. P. Bhati, D. W. Wright, A. D. Wade, G. Tresadern, H. van Vlijmen, P. V. Coveney, *Sci. Rep.* **2022**, *12*, 10433.
[58] Prefectura Naval Argentina in *Ordenanza Nº 8-98 (DPMA)*, Vol 6, Prefectura Naval Argentina, Buenos Aires, Argentina **1998**.
[59] A. S. Michael, C. G. Thompson, M. Abramovitz, *Science* **1956**, *123*, 464–464.
[60] H. D dos Santos, F. F. de Oliveira, R. A. de Oliveira, Revista Virtual de Química, **2017**, *9*, 1535–1545.
[61] P. Karunarathne, N. Pocquet, P. Labbé, P. Milesi, *Parasit. Vectors* **2022**, *15*, 35.

Entry for the Table of Contents

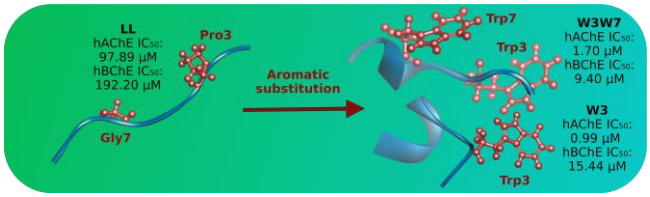

A series of peptide inhibitors of the human cholinesterase enzymes was designed by mutating aliphatic residues for aromatic ones. Trp mutations highly increased the inhibitory activity of the base sequence, and the best candidate showed the most potent activity on the human acetylcholinesterase reported for a peptide (0.99±0.02μM) and inhibited 94.2%±1.2 of the AChE-induced β-amyloid peptide aggregation.